IEEE Open Journal of the Communications Society

Received XX Month, XXXX; revised XX Month, XXXX; accepted XX Month, XXXX; Date of publication XX Month, XXXX; date of current version February 22, 2024.

Digital Object Identifier 10.1109/OJCOMS.2024.011100

Non-linear Power Harvesting and α-Fair Resource Allocation in SWIPT

Richard P. Ketcham[1] ***(Student Member, IEEE)***, **Marc Moonen** [1] ***(Fellow, IEEE)***

[1]KU Leuven, Department of Electrical Engineering (ESAT), STADIUS, Leuven, Belgium

CORRESPONDING AUTHOR: Richard P. Ketcham (e-mail: richard.ketcham@kuleuven.be).

This work was supported by: Fonds de la Recherche Scientifique - FNRS and the Fonds Wetenschappelijk Onderzoek - Vlaanderen under EOS Project no 30452698 '(MUSE-WINET) MUlti-SErvice WIreless NETwork' and FWO Research Project nr. G0C0623N "User-centric distributed signal processing algorithms for next generation cell-free massive MIMO based wireless communication networks".

ABSTRACT Power harvesting in simultaneous wireless information and power transfer (SWIPT) is known to be non-linear, but incorporating non-linear harvesting effects within the resource allocation is a non-trivial task. A practical non-linear harvesting model for SWIPT using a sigmoidal-like function has been proposed. However, sigmoidal-like functions are neither convex nor concave, so the model usually requires some transformation to make it tractable. In this paper, we propose a tractable approach to resource allocation for SWIPT with non-linear harvesting based on sigmoidal-like functions through α-fair utility functions. A method is then developed to apply the composite utility to an existing weighted sum resource allocation that relies on a linear harvesting model.

INDEX TERMS energy harvesting, fairness, multiuser, multicarrier, multiantenna, non-linear, OFDM, power harvesting, resource allocation, sigmoidal, SWIPT, time-switching, time-sharing

I. INTRODUCTION

UNLIKE traditional wireless communication networks, a simultaneous wireless information and power transfer (SWIPT) network must contend with harvesting power as well as decoding information. Many existing works consider a linear harvesting model in which the harvested power is linearly proportional to the RF power present at the receive antenna. Although recent research typically models the harvesting operation as non-linear [1], the linear model is still utilized for tractability [2]–[4]. Some authors that use the linear model cite an ability to mitigate non-linear effects by placing several power harvesting circuits in parallel to enlarge the linear power conversion region as justification [2]. However, this is not always a practical solution, so a method that can easily include non-linear harvesting effects in resource allocation for SWIPT is still important.

A practical non-linear harvesting model for SWIPT using a sigmoidal-like function was first proposed in [5]. A function $f(x)$ is sigmoidal-like if it has one inflection point x_0, with negative curvature for $x > x_0$ and positive curvature for $x < x_0$ [6]. Due to this changing curvature, the model proposed in [5] is neither convex nor concave, so directly incorporating it into an optimization problem requires additional and sometimes complex methods to solve. Indeed, works using a sigmoidal-like harvesting model resorted to several complex methods to overcome the non-convexity [5], [7]–[9]. The authors in [10] also used a sigmoidal-like utility function for bandwidth allocation in a 4G cellular network. Interestingly, [10] showed that a sigmoidal-like function encapsulated with a proportionally fair (i.e. logarithmic) utility function is strictly concave.

We seek to expand on both [5] and [10] by first providing more control over the level of fairness and then applying the resulting encapsulated sigmoidal-like function (referred to as a composite utility) to SWIPT to model non-linear power harvesting. To this end, a tractable approach to resource allocation with non-linear harvesting through a generalized set of fair utility functions, known as α-fairness, is developed. A method is then developed to apply the composite utility to an existing weighted sum resource allocation presented in [2], which relies on a linear harvesting model.

A. NOTATION

Matrices are upright and sans-serif, vectors are italicized and bold, and scalars are italicized. Sets are upright, serif, and italicized. The transpose operation is denoted with $(\cdot)^\top$,

This work is licensed under a Creative Commons Attribution 4.0 License. For more information, see https://creativecommons.org/licenses/by/4.0/

Hermitian transpose is $(\cdot)^{\mathcal{H}}$, and $\mathbb{E}[\cdot]$ is the expected value operator. The $diag(\cdot)$ operator returns a diagonal matrix with the diagonal elements given by its argument.

II. SYSTEM MODEL

Consider a SWIPT network that contains one access point and N remote devices (users), each with one antenna. Wireless transmissions are modeled as a broadcast channel (BC) in which the access point uses N_T transmit antennas to deliver data and power to the N users, where $N \leq N_T$. The network employs orthogonal frequency division multiplexing (OFDM), where the OFDM symbols are comprised of K orthogonal subcarriers. It is assumed that perfect channel state information is available and each subcarrier may be modeled independently due to the absence of inter-carrier interference.

A. BROADCAST CHANNEL

The access point applies a precoder to the symbol vector before transmitting to the users, which is modeled on each subcarrier (denoted with subscript k) as a BC with

$$\boldsymbol{y}^k = \mathsf{H}^{k\mathcal{H}}\mathsf{T}^k\boldsymbol{x}^k + \boldsymbol{z}^k. \tag{1}$$

In (1), $\boldsymbol{y}^k$ is the $N \times 1$ vector of symbols as received by the N users, $\mathsf{H}^{k\mathcal{H}}$ is the $N \times N_{\mathrm{T}}$ channel matrix, with $[\mathsf{H}^k]^{m,n\mathcal{H}}$ being the transfer function between transmit antenna m and user-n evaluated at subcarrier k, T^k is the $N_T \times N$ linear precoder matrix, $\boldsymbol{x}^k$ is the $N \times 1$ vector of transmit symbols for the N users, and $\boldsymbol{z}^k$ is an $N \times 1$ vector of additive white Gaussian noise.

B. METRICS

The downstream data rate for user-n on subcarrier k is modeled with

$$R^{k,n}(\mathsf{T}^k, \boldsymbol{s}^k) = \log_2\left(1 + \gamma^{k,n}_{\mathrm{BC}}(\mathsf{T}^k, \boldsymbol{s}^k)\right) \tag{2}$$

and the total data rate for user-n, r^n_y, is calculated by summing (2) over all subcarriers

$$r^n_y = \sum_{k=1}^{K} R^{k,n}(\mathsf{T}^k, \boldsymbol{s}^k). \tag{3}$$

The downstream signal-to-interference-plus-noise ratio (SINR) for user-n on subcarrier k, $\gamma^{k,n}_{\mathrm{BC}}(\mathsf{T}^k, \boldsymbol{s}^k)$, is a function of the precoder matrix T_k and symbol power vector $\boldsymbol{s^k}$. The n-th element of $\boldsymbol{s^k}$, denoted by $s^{k,n}$, is the symbol power for user-n. It is defined as $s^{k,n} \triangleq \mathbb{E}\left[|x^{k,n}|^2\right]$, where $x^{k,n}$ is the n-th element of $\boldsymbol{x}^k$. The SINR is given by

$$\gamma^{k,n}_{\mathrm{BC}}(\mathsf{T}^k, \boldsymbol{s}^k) = \frac{|\boldsymbol{t}^{k,n\mathcal{H}}\boldsymbol{h}^{k,n}|^2 s^{k,n}}{\sum_{\substack{m=1 \\ m\neq n}}^{N} |\boldsymbol{t}^{k,m\mathcal{H}}\boldsymbol{h}^{k,n}|^2 s^{k,m} + \sigma^{k,n}}, \tag{4}$$

where $\boldsymbol{t}^{k,n}$ is the precoder vector for user-n, i.e. the n-th column of T^k, and $\boldsymbol{h}^{k,n}$ is the transfer function for user-n, i.e. the n-th column of H^k. The additive white Gaussian noise power experienced by user-n on subcarrier k is given by $\sigma^{k,n}$.

The received power for user-n on subcarrier k is modeled with

$$P^{k,n}(\mathsf{T}^k, \boldsymbol{s}^k) = \sum_{m=1}^{N} |\boldsymbol{t}^{k,m\mathcal{H}}\boldsymbol{h}^{k,n}|^2 s^{k,m} \tag{5}$$

and the total received power for user-n, r^n_x, is calculated by summing (5) over all subcarriers

$$r^n_x = \sum_{k=1}^{K} P^{k,n}(\mathsf{T}^k, \boldsymbol{s}^k). \tag{6}$$

Similarly, the total transmit power p^n for user-n may be calculated by summing the transmit power over all subcarriers and may be modeled with

$$p^n = \sum_{k=1}^{K} s^{k,n}||\boldsymbol{t}^{k,n}||_2^2. \tag{7}$$

C. HARVESTED POWER MODEL

While [2] modeled the harvested power as linearly proportional to (6) for tractability, it has been observed that the power harvesting operation is non-linear in general [1]. A practical non-linear harvesting model for SWIPT using a sigmoidal-like function was first proposed in [5]. Here we use a normalized sigmoidal-like utility function [10] in place of [5], given as

$$U^{\sigma}(r^n_x) = c\left((1+\psi^n)^{-1} - d\right), \tag{8}$$

where

$$\begin{aligned} \psi^n &= e^{-a(r^n_x - b)} \\ c &= \frac{1+e^{ab}}{e^{ab}} \\ d &= \frac{1}{1+e^{ab}}, \end{aligned} \tag{9}$$

and r^n_x is the RF power present at the antenna for user-n as given in (6). Parameters a and b are positive and chosen experimentally, where a represents the non-linear charging rate (i.e. steepness of the curve) and b represents the minimum turn-on power [1]. Consequently, $\psi^n > 0$, $c > 0$, and $d > 0$. The harvester parameters may differ between users, but for the sake of clarity, they are assumed to be the same for all users without loss of generality (w.l.o.g).

The model satisfies $U^{\sigma}(0) = 0$ and $U^{\sigma}(\infty) = 1$. Scaling U^{σ} with the harvester saturation power, P_{SAT}, calculates the DC power produced by the harvester and is equivalent to the model proposed in [5]. The scaling with P_{SAT} is omitted here, as it is undone by the later normalization in (15) anyway. Example harvester settings are illustrated in Fig. 1. It is important to note that sigmoidal-like functions are non-convex/non-concave.

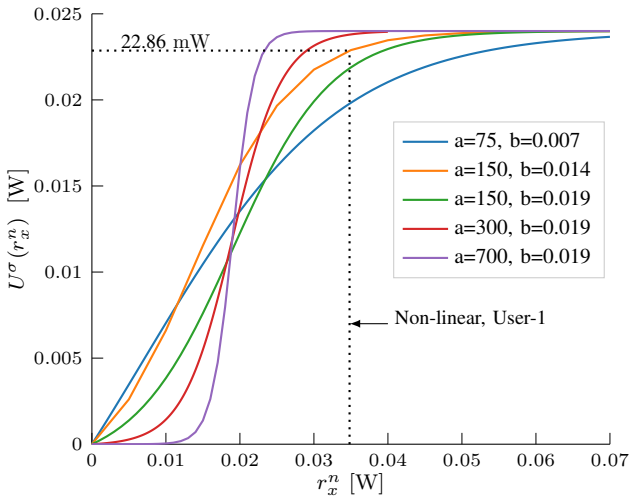

FIGURE 1. The sigmoidal-like non-linear power harvester model is illustrated here for several sets of parameters. The saturation power P_{SAT} is set to 0.024 W. Parameters $[a, b] = [150, 0.014]$ are from [8], but the rest are chosen as illustrative examples. "Non-linear, User-1" refers to the allocated power for user-1 illustrated in Fig. 5. For input power 34.8 mW, the harvester outputs 22.86 mW.

D. TIME-SWITCHING

A time-switching SWIPT receiver is considered, which performs either information decoding or power harvesting [11]. The duration for either action is determined by the time-switching ratio, given by $\alpha^n \in [0, 1]$ for user-n, where the receiver for user-n spends α^n proportion of time decoding information and $1-\alpha^n$ proportion of time harvesting power. Hence, the data rate for user-n due to time-switching is given by

$$\tilde{r}_y^n = \alpha^n r_y^n. \tag{10}$$

Similarly, the harvested power for user-n due to time-switching is given by

$$\tilde{r}_x^n = (1-\alpha^n) U^\sigma(r_x^n). \tag{11}$$

The time-switching ratios will not be optimized, i.e. will be considered constant.

III. PRIMAL PROBLEM FORMULATION

In [2], the resource allocation problem was formulated as a weighted sum of data rates subject to meeting a total transmit power constraint and individual user power harvesting constraints. In this paper, the resource allocation is generalized to incorporate fairness between objectives rather than meeting specific power harvesting constraints. In addition, instead of linear power harvesting, non-linear harvesting effects are also included.

A. α-FAIR UTILITY FUNCTION

A generalized mathematical formulation for fair resource allocation called α-fairness was proposed in [12]. α-Fairness describes a class of mostly non-linear utility functions that promote varying degrees of fairness from a weighted sum utility function (i.e. no fairness) to a max-min utility function (i.e. maximum fairness). The utility functions defined by α-fairness utilize a parameter that is usually denoted with α but will be denoted with β here to avoid confusion with the time-switching ratios. The utility functions are then defined as

$$f^\beta(\{z^n\}) = \begin{cases} \sum_{n=1}^N \mu^n \frac{(z^n)^{1-\beta}}{(1-\beta)}, & \beta \geq 0, \beta \neq 1 \\ \sum_{n=1}^N \mu^n \ln(z^n), & \beta = 1, \end{cases} \tag{12}$$

where $\{z^n\}_{\forall n}$ represents the objectives, μ^n is a weight associated with the nth objective, and β is the fairness parameter. As the fairness parameter β increases, the resource allocation becomes increasingly fair in that the resulting objectives are increasingly equivalent. Note that the natural logarithm is used for $\beta = 1$ and when $\beta = 0$, (12) reduces to a linear utility function (i.e. weighted sum utility function).

B. NORMALIZATION

With α-fairness, it is paramount to appropriately scale the objectives by the associated range of values otherwise there may be a bias. Assuming constant time-switching ratios, then the maximum power harvester utility is given by

$$U^\sigma{}_{\text{MAX}} = \max\left(\{\tilde{r}_x^n\}_{\forall n}\right) \tag{13}$$

and the maximum data rate is given by

$$R_{\text{MAX}} = \max\left(\{\tilde{r}_y^n\}_{\forall n}\right). \tag{14}$$

For user-n, the normalized harvested power and the normalized data rate are then

$$\hat{r}_x^n = \frac{\tilde{r}_x^n}{U^\sigma{}_{\text{MAX}}} \text{ and } \hat{r}_y^n = \frac{\tilde{r}_y^n}{R_{\text{MAX}}}, \tag{15}$$

respectively.

C. PRIMAL PROBLEM FORMULATION

Applying α-fairness results in the following composite utility function

$$\begin{aligned} &\beta \neq 1, \beta \geq 0: \\ &\quad \hat{f}^\beta = \sum_{n=1}^N \left(\frac{\hat{\mu}_x^n}{(\hat{r}_x^n)^{\beta-1}} + \frac{\hat{\mu}_y^n}{(\hat{r}_y^n)^{\beta-1}} \right) (1-\beta)^{-1} \\ &\beta = 1: \\ &\quad \hat{f}^\beta = \sum_{n=1}^N \hat{\mu}_x^n \ln(\hat{r}_x^n) + \hat{\mu}_y^n \ln(\hat{r}_y^n). \end{aligned} \tag{16}$$

The harvested power and data rate weights for user-n are given by $\hat{\mu}_x^n$ and $\hat{\mu}_y^n$, respectively. The weights are positive and reflect the priority of the particular user data rate and harvested power. Additionally, the weights may be denoted in vector form where an $N \times 1$ vector of harvested power weights is denoted with $\hat{\boldsymbol{\mu}}_x$ and an $N \times 1$ vector of data rate weights is denoted with $\hat{\boldsymbol{\mu}}_y$. The basic problem formulation

for the resource allocation is then given by

$$\begin{aligned} &\underset{\{\mathbf{T}^k, \boldsymbol{s}^k\}_{\forall k}}{\text{maximize}} \ \hat{f}^{\beta} \\ &\text{s.t.} \ \sum_{n=1}^{N} p^n \leq P_{\text{Total}}, \end{aligned} \tag{17}$$

where the total transmit power is constrained to be less than or equal to P_{Total}. Note that if $\alpha^n \in \{0, 1\}$ either the harvested power objective or the data rate objective for user-*n* will need to be removed from the optimization because it will be unbounded from above otherwise. This can be done by setting $\hat{\mu}_x^n = 0$ if $\alpha^n = 1$ or $\hat{\mu}_y^n = 0$ if $\alpha^n = 0$.

Problem (17) is a non-convex optimization problem due to the design parameters. Yet, provided that the utility function $\hat{f}^{\beta}$ is non-decreasing and concave, it was shown that (17) enjoys a near-zero duality gap that vanishes asymptotically as the number of subcarriers goes to ∞ [13]. This facet is known as the time-sharing property of multicarrier systems. The objective $\hat{f}^{\beta}$ is indeed shown to be strictly concave with respect to (w.r.t.) $\{r_x^n, r_y^n\}_{\forall n}$ in Proposition 1, provided that the fairness parameter β is greater than a minimum value β_{MIN}. Lemma 1 and Lemma 2 will provide the preliminaries for Proposition 1.

Lemma 1. *The gradient of $\hat{f}^{\beta}$, $\nabla \hat{f}^{\beta}$, w.r.t. the resource allocation $\{r_x^n, r_y^n\}_{\forall n}$ is comprised of the partial derivatives given as*

$$\begin{aligned} \frac{\partial \hat{f}^{\beta}}{\partial r_x^n} &= \frac{\hat{\mu}^n}{(\hat{r}_x^n)^{\beta}} \cdot \frac{1-\alpha^n}{U^{\sigma}{}_{MAX}} \cdot \frac{ca\psi^n}{(1+\psi^n)^2} \\ \frac{\partial \hat{f}^{\beta}}{\partial r_y^n} &= \frac{\hat{\mu}_y^n}{(\hat{r}_y^n)^{\beta}} \cdot \frac{\alpha^n}{R_{MAX}} \end{aligned} \tag{18}$$

for all n and for $\beta \geq 0$. In addition, $\hat{f}^{\beta}$ is non-decreasing.

Proof:
The partial derivative of ψ^n, defined in (9), is

$$\frac{\partial}{\partial r_x^n} \psi^n = -a\psi^n, \tag{19}$$

so the partial derivative of $U^{\sigma}(r_x^n)$, defined in (8), is

$$\frac{\partial}{\partial r_x^n} U^{\sigma}(r_x^n) = \frac{ca\psi^n}{(1+\psi^n)^2}. \tag{20}$$

For $\beta \geq 0$ and $\beta \neq 1$, the partial derivatives of $\hat{f}^{\beta}$ w.r.t. r_x^n and r_y^n are

$$\begin{aligned} \frac{\partial}{\partial r_x^n} \hat{f}^{\beta} &= \frac{\partial}{\partial \hat{r}_x^n} \hat{f}^{\beta} \cdot \frac{\partial}{\partial r_x^n} \hat{r}_x^n \\ &= \frac{\hat{\mu}^n}{(\hat{r}_x^n)^{\beta}} \cdot \frac{1-\alpha^n}{U^{\sigma}{}_{\text{MAX}}} \cdot \frac{ca\psi^n}{(1+\psi^n)^2} \\ \frac{\partial}{\partial r_y^n} \hat{f}^{\beta} &= \frac{\hat{\mu}_y^n}{(\hat{r}_y^n)^{\beta}} \cdot \frac{\alpha^n}{R_{\text{MAX}}}. \end{aligned} \tag{21}$$

The utility function for $\beta = 1$ is given in (16), the partial derivatives of which result in the same expressions given in (21). Note that the partial derivatives are all non-negative, meaning that $\hat{f}^{\beta}$ is a non-decreasing function. ■

Lemma 2. *The Hessian of $\hat{f}^{\beta}$, $\nabla^2 \hat{f}^{\beta}$, w.r.t. the resource allocation $\{r_x^n, r_y^n\}_{\forall n}$ is a diagonal matrix, with the diagonal entries given in* (25) *and* (26)*.*

Proof:
The partial derivative w.r.t. r_x^n in (21) can be put in terms of ψ^n using the definition of $U^{\sigma}(r_x^n)$ in (8)

$$\begin{aligned} \frac{\partial}{\partial r_x^n} \hat{f}^{\beta} &= \frac{\hat{\mu}^n}{(\hat{r}_x^n)^{\beta}} \cdot \frac{1-\alpha^n}{U^{\sigma}{}_{\text{MAX}}} \cdot \frac{ca\psi^n}{(1+\psi^n)^2} \\ &= \frac{\hat{\mu}_x^n}{\left(\frac{(1-\alpha^n)c}{U^{\sigma}{}_{\text{MAX}}}((1-\psi^n)^{-1} - d)\right)^{\beta}} \cdot \frac{ca\psi^n(1-\alpha^n)}{U^{\sigma}{}_{\text{MAX}}(1+\psi^n)^2} \\ &= \frac{\hat{\mu}_x^n a}{\left(\frac{(1-\alpha^n)c}{U^{\sigma}{}_{\text{MAX}}}\right)^{\beta-1}} \cdot \frac{(1+\psi^n)^{\beta-2}\psi^n}{(1-d(1+\psi^n))^{\beta}}. \end{aligned} \tag{22}$$

Let

$$\begin{aligned} A &= (1+\psi^n)^{\beta-2}\psi^n \\ B &= (1-d(1+\psi^n))^{-\beta}, \end{aligned} \tag{23}$$

then

$$\begin{aligned} \frac{\partial}{\partial r_x^n} A &= -a\psi^n \left((1+\psi^n)^{\beta-2} + \psi^n(\beta-2)(1+\psi^n)^{\beta-3}\right) \\ \frac{\partial}{\partial r_x^n} B &= -a\psi^n \left(d\beta(1-d(1+\psi^n))^{-\beta-1}\right). \end{aligned} \tag{24}$$

Through the product rule, the second partial derivative w.r.t. r_x^n is given by

$$\begin{aligned} \frac{\partial^2}{\partial r_x^n \partial r_x^n} \hat{f}^{\beta} &= \frac{\hat{\mu}_x^n a}{\left(\frac{(1-\alpha^n)c}{U^{\sigma}{}_{\text{MAX}}}\right)^{\beta-1}} \left(\frac{\partial A}{\partial r_x^n} B + \frac{\partial B}{\partial r_x^n} A\right) \\ &= \frac{-\hat{\mu}_x^n a^2 \psi^n (1+\psi^n)^{\beta-2}}{\left(\frac{(1-\alpha^n)c}{U^{\sigma}{}_{\text{MAX}}}\right)^{\beta-1}} \Bigg[\frac{d\beta\psi^n}{(1-d(1+\psi^n))^{\beta+1}} \\ &\quad + \frac{1}{(1-d(1+\psi^n))^{\beta}} + \frac{(\beta-2)\psi^n}{(1+\psi^n)(1-d(1+\psi^n))^{\beta}}\Bigg]. \end{aligned} \tag{25}$$

The second partial derivative w.r.t. r_y^n is

$$\frac{\partial^2}{\partial r_y^n \partial r_y^n} \hat{f}^{\beta} = \frac{-\beta\hat{\mu}_y^n}{(\hat{r}_y^n)^{\beta+1}} \left(\frac{\alpha^n}{R_{\text{MAX}}}\right)^2. \tag{26}$$

Lastly, observe that the partial derivatives w.r.t. r_x do not depend on r_y and vice versa, nor do the partial derivatives for user-*n* depend on user-*j* for $n \neq j$. Hence,

$$\begin{aligned} \frac{\partial^2}{\partial r_x^n \partial r_x^j} \hat{f}^{\beta} &= 0 \ \forall \ n \neq j \\ \frac{\partial^2}{\partial r_y^n \partial r_y^j} \hat{f}^{\beta} &= 0 \ \forall \ n \neq j \\ \frac{\partial^2}{\partial r_x^n \partial r_y^j} \hat{f}^{\beta} &= 0 \ \forall n, j \in [1, N]. \end{aligned} \tag{27}$$

Since all terms are 0 except for those on the main diagonal, the Hessian is a diagonal matrix. ■

Proposition 1. *The composite utility function described in* (16) *is strictly concave w.r.t.* $\{r_x^n, r_y^n\}_{\forall n}$ *for* $\beta > \beta_{MIN} = 1 - \frac{2\sqrt{e^{ab}}}{1+e^{ab}}$.

Proof:

The received RF power for user-n, r_x^n, is non-negative. For non-negative values, the sigmoidal-like utility function can be bounded [10] with

$$\begin{aligned} &0 \leq U^{\sigma}(r_x^n) \leq 1 \\ &0 \leq c((1+\psi^n)^{-1} - d) \leq 1 \\ &d \leq (1+\psi^n)^{-1} \leq \frac{1+cd}{c}. \end{aligned} \tag{28}$$

Inverting and rearranging, we arrive at

$$\begin{aligned} &\frac{1}{d} \geq (1+\psi^n) \geq \frac{c}{1+cd} \\ &0 \geq d(1+\psi^n) - 1 \geq \frac{cd}{1+cd} - \frac{1+cd}{1+cd} \\ &0 \leq 1 - d(1+\psi^n) \leq \frac{1}{1+cd}. \end{aligned} \tag{29}$$

Lemma 2 showed that $\nabla^2 \hat{f}^{\beta}$ is a diagonal matrix, so it is strictly concave when all of the diagonal entries, defined by (25) and (26), are negative. The diagonal entries described in (26) are negative for all $\beta > 0$. The diagonal entries described in (25) are negative if

$$\begin{aligned} &\frac{d\beta\psi^n}{(1-d(1+\psi^n))^{\beta+1}} + \frac{1}{(1-d(1+\psi^n))^{\beta}} \\ &+ \frac{(\beta-2)\psi^n}{(1+\psi^n)(1-d(1+\psi^n))^{\beta}} > 0. \end{aligned} \tag{30}$$

Note that since $d > 0$, $\psi^n > 0$, and $(1-d(1+\psi)) \geq 0$ from (29), it is immediately clear that (25) is negative for $\beta \geq 2$. Finding the common denominator of (30) and multiplying through, we arrive at

$$\begin{aligned} &(\beta-2)\psi^n(1-d(1+\psi^n))+ \\ &(1+\psi^n)(1-d(1+\psi^n)) + d\beta\psi^n(1+\psi^n) > 0. \end{aligned} \tag{31}$$

Solving for β, we arrive at

$$\beta > (1-\psi^{n^{-1}})(1-d(1+\psi^n)) = g(r_x^n). \tag{32}$$

Thus, $\hat{f}^{\beta}$ is strictly concave as long as β is greater than $g(r_x^n)$ for all values of $r_x^n \geq 0$, i.e.

$$\beta > \max_{r_x^n \geq 0} g(r_x^n). \tag{33}$$

Let us solve for the value of r_x^n that yields the largest lower bound β_{MIN} for β. Distributing terms

$$\begin{aligned} g(r_x^n) &= (1-\psi^{n^{-1}})(1-d(1+\psi^n)) \\ &= (1-\psi^{n^{-1}}) - d(\psi^n - \psi^{n^{-1}}) \\ &= 1 - \psi^{n^{-1}}(1-d) - d\psi^n, \end{aligned} \tag{34}$$

$g(r_x^n)$ can be shown to be concave by first taking the first derivative

$$\begin{aligned} \frac{\partial}{\partial r_x^n} g(r_x^n) &= \frac{\partial}{\partial \psi^n} g(r_x^n) \frac{\partial}{\partial r_x^n} \psi^n \\ &= (\psi^{n^{-2}}(1-d) - d)(-a\psi^n) \\ &= ad\psi^n - a\psi^{n^{-1}}(1-d) \end{aligned} \tag{35}$$

and then the second derivative

$$\frac{\partial^2}{\partial {r_x^n}^2} g(r_x^n) = -(a^2\psi^{n^{-1}}(1-d) + a^2 d\psi^n) < 0. \tag{36}$$

Since a is positive and real, $\psi > 0$, and $(1-d) > 0$, the second derivative is negative and is thus strictly concave. Hence, we can solve for the unique value of r_x^n that yields the largest $g(r_x^n)$ by setting the first derivative (35) to 0

$$\begin{aligned} ad\psi^n - a\psi^{n^{-1}}(1-d) &= 0 \\ \psi^{n^2} &= \frac{1-d}{d} \\ \psi^n &= \sqrt{1+e^{ab}-1} \\ e^{-ar_x^n} e^{ab} &= \sqrt{e^{ab}} \\ r_x^n &= \frac{\ln\left(\sqrt{e^{-ab}}\right)}{-a}. \end{aligned} \tag{37}$$

Note that $0 < \sqrt{e^{-ab}} < 1$, so $\ln\left(\sqrt{e^{-ab}}\right) < 0$ and $r_x^n > 0$. Substituting (37) into (32), we arrive at the following bound β_{MIN} for strict concavity

$$\begin{aligned} \beta_{\text{MIN}} &= g\left(\ln\left(\sqrt{e^{-ab}}\right)(-a)^{-1}\right) \\ &= 1 - \sqrt{e^{ab}}^{-1}(1-d) - d\sqrt{e^{ab}} \\ &= 1 - \frac{2e^{ab}}{\sqrt{e^{ab}}(1+e^{ab})} \\ &= 1 - \frac{2\sqrt{e^{ab}}}{1+e^{ab}}. \end{aligned} \tag{38}$$

■

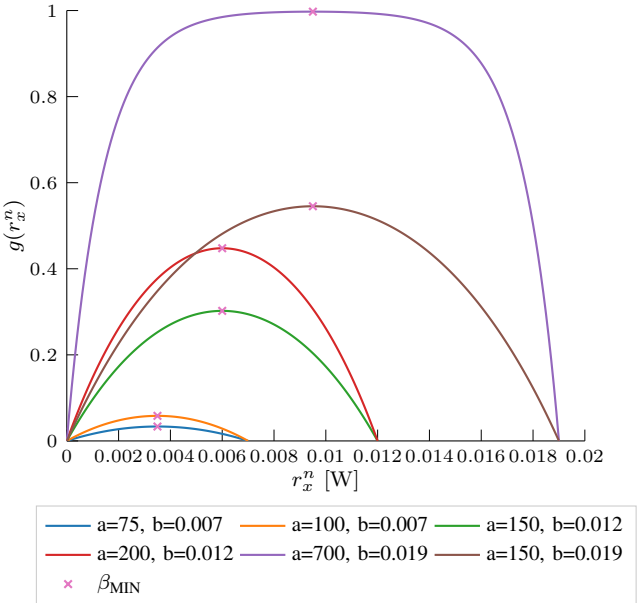

FIGURE 2. $g(r_x^n)$ **is graphed as a function of** r_x^n **and various model parameters. Observe that** β_{MIN} **is the maximum value of** $g(r_x^n)$**. Setting** $\beta > \beta_{\text{MIN}}$ **will make** $\hat{f}^{\beta}$ **strictly concave for all values of** r_x^n**.**

Fig. 2 illustrates $g(r_x^n)$. Setting $\beta > \beta_{\text{MIN}}$ will make $\hat{f}^\beta$ strictly concave for all values of r_x^n. As (38) indicates, the bound is not dependent on r_x^n, but on the harvester parameters. Provided that all users have the same harvester parameters, then all users will have the same β_{MIN}. Fig. 3 illustrates that the composite utility is non-concave for $\beta < \beta_{\text{MIN}}$. Conversely, Fig. 4 illustrates that the composite utility is concave for $\beta > \beta_{\text{MIN}}$. Note that each trace in Fig. 3 is scaled by $\max|f^\beta(U^\sigma(r_x^n))|$ to better compare the curvatures. The traces in Fig. 4 are not scaled since they are all clearly concave.

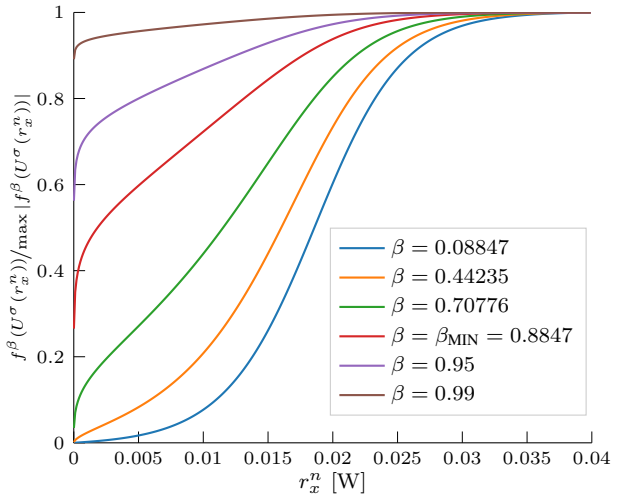

FIGURE 3. Observe that $f^\beta(U^\sigma(r_x^n))$ is non-concave for $\beta < \beta_{\text{MIN}}$ and concave for $\beta > \beta_{\text{MIN}}$. Note that $f^\beta(U^\sigma(r_x^n))$ is positive for $\beta < 1$. The parameters used for this plot are $a = 300$ and $b = 0.019$.

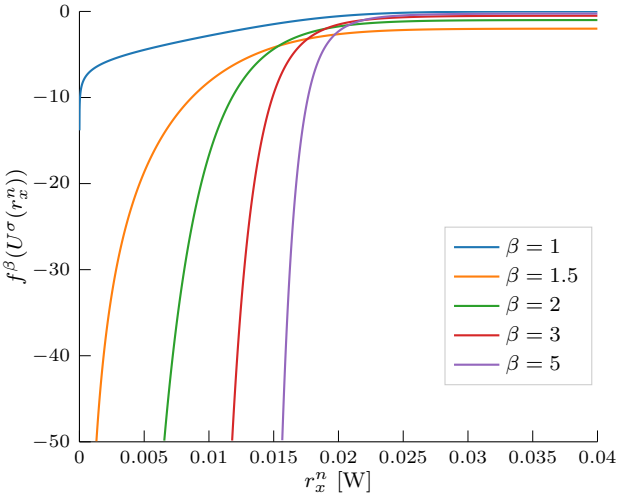

FIGURE 4. Observe that the $f^\beta(U^\sigma(r_x^n))$ is concave for $\beta \geq 1$. The parameters used for this plot are $a = 300$ and $b = 0.019$.

D. LINEARIZATION

It is not possible to directly solve a sum-rate maximization in the BC due to non-convexities introduced by the physical parameters [14]. However, [2] managed to solve it indirectly via dual decomposition, a multiple access channel (MAC)-BC duality, and successive convex approximation (SCA). Many of the challenges addressed in [2] are also considered here. Unfortunately, (17) compounds these by adding a non-convex/non-concave power harvesting model and encapsulating the user objectives in α-fairness utility functions, which ostensibly precludes applying the solution methods developed in [2] directly to the problem considered here.

Since $\hat{f}^\beta$ is strictly concave for an appropriate β and the domain is convex due to time-sharing [13], [15], (17) can be solved through the conditional gradient method [16] by linearizing (16) and maximizing iteratively. The partial derivative of (16) is given in Lemma 1. The linearized objective is then expressed as

$$\begin{aligned}\hat{f}^\beta_{\text{lin}} &\triangleq \sum_{n=1}^{N} \left.\frac{\partial f^\beta}{\partial r_x^n}\right|_{\bar{r}_x^n} (r_x^n - \bar{r}_x^n) + \left.\frac{\partial f^\beta}{\partial r_y^n}\right|_{\bar{r}_y^n} (r_y^n - \bar{r}_y^n) \\ &\quad + \hat{f}^\beta\left(\{\bar{r}_x^n, \bar{r}_y^n\}_{\forall n}\right) \\ &= \sum_{n=1}^{N} \frac{\hat{\mu}^n}{(\bar{r}_x^n)^\beta} \frac{ca\bar{\psi}^n}{(1+\bar{\psi}^n)^2} \frac{1-\alpha^n}{U^\sigma{}_{\text{MAX}}} r_x^n + \frac{\hat{\mu}_y^n}{(\bar{r}_y^n)^\beta} \frac{\alpha^n}{R_{\text{MAX}}} r_y^n \\ &\quad + \text{Constant}\end{aligned} \tag{39}$$

where $\{\bar{r}_x^n, \bar{r}_y^n\}_{\forall n}$ is the set of rates and $\{\bar{\psi}^n\}_{\forall n}$ is the set of values for $\{\psi^n\}_{\forall n}$ achieved in the previous iteration. "Constant" represents all terms that are independent of $\{r_x^n, r_y^n\}_{\forall n}$ and so are constant. If these sets are updated according to

$$\begin{aligned}\ddot{r}^n_{y_{i+1}} &= (1-\gamma_i)\ddot{r}^n_{y_i} + \gamma_i r^n_{y_i} \\ \ddot{r}^n_{x_{i+1}} &= (1-\gamma_i)\ddot{r}^n_{x_i} + \gamma_i r^n_{x_i}\end{aligned} \tag{40}$$

and

$$\begin{aligned}\bar{\psi}^n_{i+1} &= e^{-a(\ddot{r}^n_{x_{i+1}} - b)} \\ \bar{r}^n_{y_{i+1}} &= \frac{\alpha^n}{R_{\text{MAX}}} \ddot{r}^n_{y_{i+1}} \\ \bar{r}^n_{x_{i+1}} &= \frac{(1-\alpha^n)}{U^\sigma{}_{\text{MAX}}} U^\sigma(\ddot{r}^n_{x_{i+1}})\end{aligned} \tag{41}$$

while the step size γ is adjusted according to $\gamma_i = 2/2+i$, then convergence is guaranteed [16]. Note that $\{r^n_{x_i}, r^n_{y_i}\}_{\forall n}$ is the solution in the ith iteration and $\{\ddot{r}^n_{x_{i+1}}, \ddot{r}^n_{y_{i+1}}\}_{\forall n}$ is the $(i+1)^{\text{th}}$ value defined by the exponential average in (40). Observe that for $i = 0$, $\gamma = 1$ and

$$\begin{aligned}\ddot{r}^n_{y_1} &= r^n_{y_0} \\ \ddot{r}^n_{x_1} &= r^n_{x_0}.\end{aligned} \tag{42}$$

Replacing $\hat{f}^\beta$ with $\hat{f}^\beta_{\text{lin}}$ in (17) and omitting the constant terms produces a problem that looks markedly like a weighted sum of rate and power maximization (WSRPM). Hence, the linearization enables interpreting the problem as

a weighted sum given by

$$\begin{aligned} \underset{\{\mathsf{T}^k,\boldsymbol{s}^k\}_{\forall k}}{\text{maximize}} \; & \sum_{n=1}^{N} \hat{w}_x^n(1-\alpha^n)r_x^n + \hat{w}_y^n\alpha^n r_y^n \\ \text{s.t.} \; & \sum_{n}^{N} p^n \leq P_{\text{Total}} \end{aligned} \tag{43}$$

with weights

$$\begin{aligned} \hat{w}_x^n &= \frac{\hat{\mu}^n}{(\bar{r}_x^n)^\beta}\frac{ca\psi}{(1+\psi)^2}\frac{1}{U^{\sigma}{}_{\text{MAX}}} \\ \hat{w}_y^n &= \frac{\hat{\mu}_y^n}{(\bar{r}_y^n)^\beta}\frac{1}{R_{\text{MAX}}}, \end{aligned} \tag{44}$$

for all users n.

IV. DUAL PROBLEM

Casting (17) as the weighted sum in (43) enables utilizing the reasoning and methods developed in [2]. First, enabled by the time-sharing property of multicarrier systems, (43) can be solved to *near optimality* through Lagrange duality.

A. DUAL PROBLEM FORMULATION

The dual problem is formed by dualizing the total power constraint. The Lagrange dual function is defined as

$$q(\lambda) \triangleq \max_{\mathsf{T},\mathsf{s}} \mathcal{L}(\mathsf{s},\mathsf{T},\lambda) \tag{45}$$

where λ is the Lagrange multiplier for the total power constraint and $\mathcal{L}(\mathsf{s},\mathsf{T},\lambda)$ is the Lagrangian. The Lagrangian may be expressed as

$$\mathcal{L}(\mathsf{s},\mathsf{T},\lambda) \triangleq \lambda P_{\text{Total}} + \sum_{k=1}^{K} \mathcal{L}^k(\boldsymbol{s}^k,\mathsf{T}^k,\lambda), \tag{46}$$

where

$$\begin{aligned} \mathcal{L}^k(\boldsymbol{s}^k,\mathsf{T}^k,\lambda) = & \sum_{n=1}^{N} \hat{w}_y^n\alpha^n R^{k,n}(\mathsf{T}^k,\boldsymbol{s}^k) - \\ & \sum_{n=1}^{N} \boldsymbol{t}^{k,n\,\mathcal{H}}\Upsilon^k(\lambda)\boldsymbol{t}^{k,n}s^{k,n} \end{aligned} \tag{47}$$

and

$$\Upsilon^k(\lambda) \triangleq \left(\lambda I - \sum_{m=1}^{N} \hat{w}_x^m(1-\alpha^m)\boldsymbol{h}^{k,m}\boldsymbol{h}^{k,m\,\mathcal{H}}\right). \tag{48}$$

The Lagrange dual problem is then given by

$$\begin{aligned} \underset{\lambda}{\text{minimize}} \; & q(\lambda) \\ \text{s.t.} \; & \lambda \geq 0 \\ & \Upsilon^k(\lambda) \succ 0 \; \forall k, \end{aligned} \tag{49}$$

where the constraint on Υ^k bounds the dual problem from below.

B. SOLVING THE DUAL PROBLEM

Observe that (49) is essentially the same as the dual problem developed in [2], where $\hat{w}_x^n$ replaces the Lagrange multiplier λ_n and $\hat{w}_y^n$ replaces ω_n for all users n, and individual harvesting constraints are omitted. As such, the same methods, namely MAC-BC duality and SCA, can be used to solve for the power allocation and precoders. The optimization is non-convex in the dual MAC however, so only a local optimum can be guaranteed. The reader is referred to [2] for further details.

Despite the similarities, there are two differences. For one, only a bi-section is required to adjust the Lagrange multiplier λ for the total transmit power constraint. Due to the constraint on $\Upsilon^k(\lambda)$, the lower bound λ_{MIN} for λ is given by the maximum eigenvalue of $\mathsf{H}^{k\,\mathcal{H}}diag(\hat{\boldsymbol{w}}_x(1-\boldsymbol{\alpha}))\mathsf{H}^k$ over all subcarriers k. The upper bound λ_{MAX} for λ is any value greater than λ_{MIN} that causes (49) to satisfy the total transmit power constraint, e.g.

$$\sum_{n=1}^{N} p^n \leq P_{\text{Total}}. \tag{50}$$

λ_{MAX} can be found by iteratively solving (49) while simultaneously increasing (e.g. doubling) λ until the total transmit power constraint is satisfied, starting with $\lambda > \lambda_{\text{MIN}}$. Once the bounds are found, a bisection is used to find the optimal value for λ. Second, an additional loop is required to iteratively solve the linearized objective. Algorithm 1 describes the optimization procedure using the SCA in [2] with the weights modified as discussed.

V. COMMENTS ON GENERAL APPLICATION

As noted, U^σ is not convex nor concave, so directly incorporating it into an optimization would require additional and sometimes complex methods to solve. However, encapsulating the harvesting model in an α-fair utility function offers an easy alternative for including non-linear power harvesting effects in general resource allocation algorithms for SWIPT. The linearization of the composite utility w.r.t. to the underlying resource allocation results in a WSRPM as demonstrated in (39) and, since the linearization is agnostic to the system model and methods used to determine $\{r_x^n, r_y^n\}_{\forall n}$, it can be applied generically.

Moreover, Proposition 1 proves that the composite utility is strictly concave for $\beta > 1 - 2\sqrt{e^{ab}}(1+e^{ab})^{-1}$, which has two consequences. First, for an appropriate β, the level of optimality is dictated by the underlying method for determining the data rates and received power $\{r_x^n, r_y^n\}_{\forall n}$ and not by the non-convex/non-concave harvesting model. Second, since $2\sqrt{e^{ab}}(1+e^{ab})^{-1} > 0$, the $\max(\beta_{\text{MIN}}) < 1$, so the most amount of fairness required for the situation is approximately proportionally fair or $\beta = 1$. With convenient values of a and b, the fairness criterion may be reduced further. Also, note that it is possible to have different fairness values based on the objective, so $\beta_y > 0$ could be used for

Algorithm 1 α-Fair Resource Allocation

Choose $\alpha_n \in [0,1]\ \forall\ n$, $\{\hat{\mu}_x^n, \hat{\mu}_y^n\}_{\forall n}$, and $\beta > \beta_{\text{MIN}}$
Choose convergence tolerances ϵ_p ϵ_β
$i = 0, \hat{\boldsymbol{w}}_{x_i} = \hat{\boldsymbol{\mu}}_x$, $\hat{\boldsymbol{w}}_{y_i} = \hat{\boldsymbol{\mu}}_y$
Initialize $\{\bar{r}_{x_i}^n, \bar{r}_{y_i}^n\}_{\forall n} = 0$
while true **do** ▷ Linearized Objective
  Choose $\lambda_{\text{MIN}}, \lambda_{\text{MAX}}$
  $j = 0$, $\Delta_p = \infty$
  while $\Delta_p \geq \epsilon_p$ **do** ▷ Total Power Constraint
    $\lambda_j = (\lambda_{\text{MAX}} - \lambda_{\text{MIN}})/2$
    $\{\mathsf{T}_j, \mathsf{s}_j\} = \text{SCA}(\hat{\boldsymbol{w}}_{x_i}, \hat{\boldsymbol{w}}_{y_i}, \lambda_j, \mathbf{H}, \boldsymbol{\sigma})$ from [2]
    Calculate $p_j^n\ \forall n$ with (7) then $P_j = \sum_n^N p_j^n$
    if $P_j < P_{\text{Total}}$ **then**
      $\lambda_{\text{MAX}} = \lambda_j$
    else
      $\lambda_{\text{MIN}} = \lambda_j$
    $\Delta_p = {}^{|P_j - P_{\text{Total}}|}/_{P_{\text{Total}}}$, $j = j + 1$
  Generate $\{r_{x_i}^n, r_{y_i}^n\}_{\forall n}$ using (3) and (6)
  Update $\gamma_i = {}^2/_{2+i}$
  Update $\ddot{\boldsymbol{r}}_{i+1} = \{\ddot{r}_{x_{i+1}}^n, \ddot{r}_{y_{i+1}}^n\}_{\forall n}$ using (40)
  if $\|\frac{\ddot{\boldsymbol{r}}_{i+1} - \ddot{\boldsymbol{r}}_i}{\ddot{\boldsymbol{r}}_{i+1} + \ddot{\boldsymbol{r}}_i}\| \leq \epsilon_\beta$ **then**
    return $\{\hat{\boldsymbol{w}}_{x_i}, \hat{\boldsymbol{w}}_{y_i}, \{r_{x_i}^n, r_{y_i}^n\}_{\forall n}, \mathsf{T}_i, \mathsf{s}_i, P_i, \lambda_i\}$
  Update $\{\bar{r}_{x_{i+1}}^n, \bar{r}_{y_{i+1}}^n\}_{\forall n}$ and $\{\bar{\psi}_{i+1}^n\}_{\forall n}$ using (41)
  $i = i + 1$
  Calculate $\hat{\boldsymbol{w}}_{x_i}$, $\hat{\boldsymbol{w}}_{y_i}$ from (44)

the data rates while $\beta_x > 1 - 2\sqrt{e^{ab}}(1+e^{ab})^{-1}$ for harvested power.

VI. SIMULATIONS

The parameters used for the following simulations are listed in Table 1. Note that only one set of time-switching ratios is used since they are constant and the particular values merely limit the range of user data rates and harvested powers. Only two users are simulated for clarity of exposition, and since a two-user network is enough to make the problem non-convex. The reader is referred to [2] for simulations with $N > 2$ using the underlying resource allocation.

The non-linear power harvesting model has a saturation point where additional input power will not increase the output power, as is illustrated in Fig. 1 for various harvesting parameters. For the harvesting parameters listed in Table 1, Fig. 1 shows that the output power transitions to saturation when r_x^n is between 25 and 40 mW and maximum output power is 24 mW. The transition to saturation increasingly limits the usefulness of allocating additional power, so the allocated power is expected to be limited to this range for each user.

For the parameters in Table 1 with $\hat{\boldsymbol{\mu}}_x = [10,1]^\top$ and $\hat{\boldsymbol{\mu}}_y = [1,1]^\top$, the impact of the harvesting model on the received power for each user is illustrated in Fig. 5. Observe that the non-linear harvesting model produces a higher subcarrier power allocation than the linear harvesting

TABLE 1. Simulation Parameters

Parameter	Value
First Subcarrier Frequency, f_0	915 MHz
Number of Subcarriers,K	64
Subcarrier Bandwidth	312500 Hz
OFDM Bandwidth	20 MHz
Total Power Constraint, P_{Total}	30 dBm
Large Scale Path Loss	30.26, 27.23 dB
Number of Transmit Antennas, N_{T}	10
Number of Users, N	2
Time-Switching Ratio, α^n	0.5
Fading Environment	Rician
Noise Power Density, σ	-112 dBm/Hz
Saturation Power, P_{SAT}	0.024 W
a	150
b	0.014 W
Convergence Tolerance, ϵ_β	$1e-4$
Convergence Tolerance, ϵ_p	$1e-7$

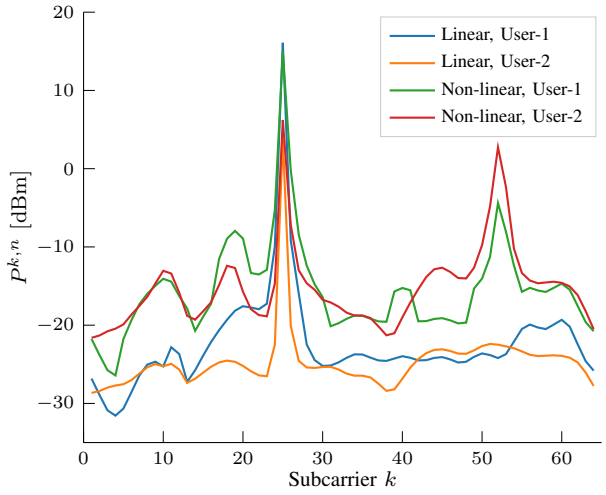

FIGURE 5. The impact of the harvesting model on received power for each user is illustrated here. The fairness parameter is $\beta = 0.3802$. Note that $\beta > \beta_{\text{MIN}} = 0.3764$. The weights were set to promote high harvested power for user-*1* with $\hat{\boldsymbol{\mu}}_x = [10,1]^\top$ and $\hat{\boldsymbol{\mu}}_y = [1,1]^\top$. A reduced path loss of 27.23 dB is used to ensure the non-linear power harvester can be saturated.

model for all subcarriers except for $k = 25$, which is where the peak power allocation for both models occurs. With the linear model, user-*1* is allocated 16.08 dBm and user-*2* is allocated 3.762 dBm on $k = 25$. With the non-linear model, user-*1* is allocated 14.94 dBm and user-*2* is allocated 6.22 dBm on $k = 25$. Summing over all subcarriers and converting to mW, user-*1* is allocated 34.8 mW in the non-

linear harvesting case, while 41.18 mW is allocated in the linear case.

Clearly, the non-linear model limits the power allocated to any one user and redistributes the excess power to increase the harvested power of user-*2* as well as the data rates (e.g. data rates increase with increasing SINR) for both users. This limit is due to the saturation of the harvester as noted earlier. The non-linear received power for user-*1* is illustrated in Fig. 1, which shows the resulting harvested power is 22.86 mW and is near the 24 mW maximum. In comparison, the linear received power for user-*1* produces 23.5 mW of harvested power, which requires increasing received power by 18% to increase harvested power by a mere 2.8%.

Setting the weights to support high data rate for user-*2* with $\hat{\boldsymbol{\mu}}_x = [1,1]^\top$ and $\hat{\boldsymbol{\mu}}_y = [1,1000]^\top$, Fig. 6, 7, and 8 show the impact of the fairness parameter β on the fairness of the resource allocation, harvested power, and the data rate, respectively. Fairness is measured using Jain's fairness index [17]. There are $2N$ objectives, so the index ranges from $\frac{1}{2N}$ to 1, where 1 means all users have the same allocation. As expected, fairness increases with β in Fig. 6. Harvested power became increasingly equitable between the users as β increased in Fig. 7. Likewise, in Fig. 8 the data rates became increasingly equitable as β increased. In particular, the data rate for user-*1* increased while the data rate for user-*2*, which the weights promoted, decreased marginally.

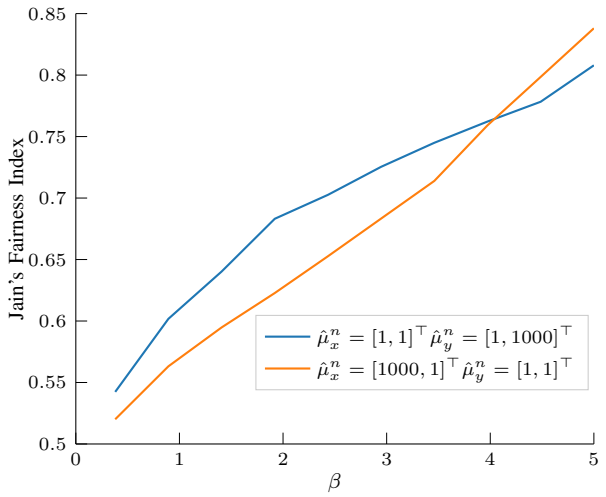

FIGURE 6. Fairness, given by Jain's fairness index [17], is seen here to increase in tandem with the fairness parameter. The path loss is set to 30.26 dB.

Setting the weights to support high harvested power for user-*1* with $\hat{\boldsymbol{\mu}}_x = [1000,1]^\top$ and $\hat{\boldsymbol{\mu}}_y = [1,1]^\top$, Fig. 6, 9, and 10 show the impact of the fairness parameter β on the fairness of the resource allocation, harvested power, and the data rate, respectively. Observe that fairness increases with β in Fig. 6. Interestingly the data rates in Fig. 10 maintained the same relative equity for most values of β but increased in value simultaneously with an increasing β. In Fig. 9, the harvested power for user-*2* increased with an

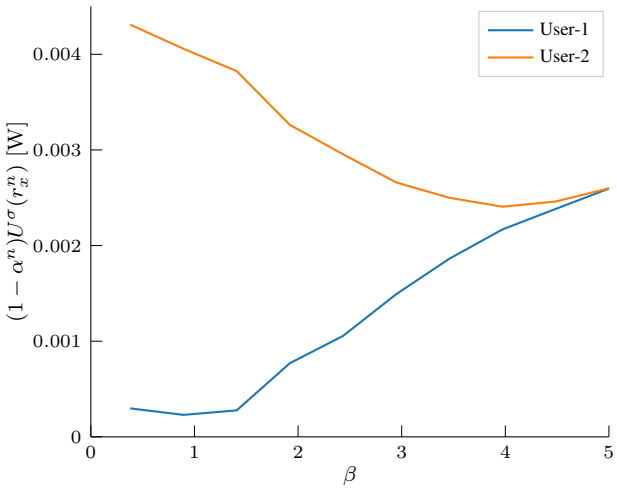

FIGURE 7. Observe that the time-switched harvested power between users becomes increasingly equitable as the fairness parameter increases. The weights are set to promote high data rate with $\hat{\boldsymbol{\mu}}_x = [1,1]^\top$ and $\hat{\boldsymbol{\mu}}_y = [1,1000]^\top$ for all users n. The path loss is set to 30.26 dB.

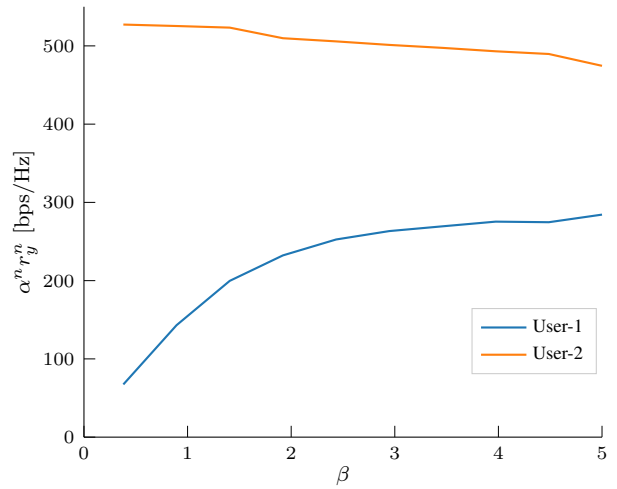

FIGURE 8. The time-switched data rate becomes increasingly equitable as the fairness parameter increases. The weights are set to promote high data rate with $\hat{\boldsymbol{\mu}}_x = [1,1]^\top$ and $\hat{\boldsymbol{\mu}}_y = [1,1000]^\top$ for all users n. The path loss is set to 30.26 dB.

increasing β, while the harvested power for user-*1*, which the weights promoted, decreased with β. Hence, Fig. 9 showed increasing equity between users as β increased.

VII. CONCLUSION

In this paper, we have considered a practical model for non-linear power harvesting in a SWIPT network. The model utilizes a sigmoidal-like function which is neither convex nor concave. Due to the non-concavity, the model cannot be directly added to an optimization without additional transformations to make it concave. To improve the tractability of its use, we have proposed utilizing α-fairness to encapsulate and concavify the power harvesting model. It has been shown that the composite utility is strictly concave for

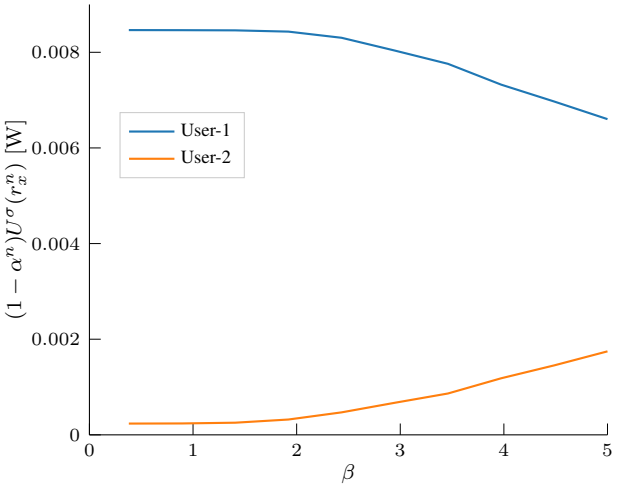

FIGURE 9. The time-switched harvested power becomes increasingly equitable as the fairness parameter increases. The weights were set to promote high harvested power with $\hat{\boldsymbol{\mu}}_x = [1000, 1]^\top$ and $\hat{\boldsymbol{\mu}}_y = [1, 1]^\top$ for all users n. The path loss is set to 30.26 dB.

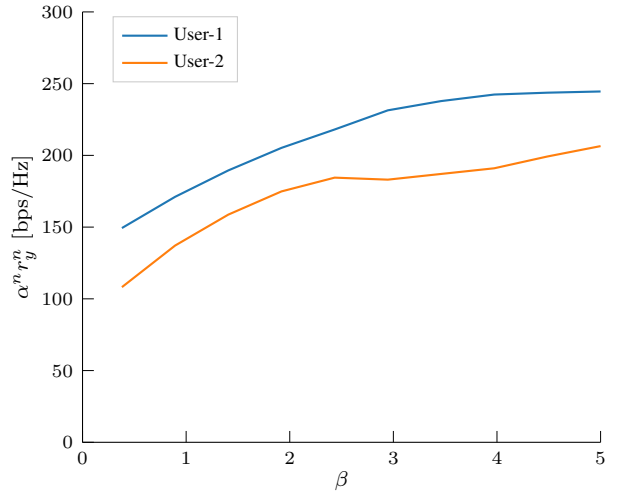

FIGURE 10. The time-switched data rate increases with an increasing fairness parameter. The weights were set to promote high harvested power with $\hat{\boldsymbol{\mu}}_x = [1000, 1]^\top$ and $\hat{\boldsymbol{\mu}}_y = [1, 1]^\top$ for all users n. The path loss is set to 30.26 dB.

fairness parameters greater than a certain value related to the harvesting model. This improves on [10] by enabling a much wider range of fairness, including levels of fairness that are less fair than required in [10]. Strict concavity enables including non-linear harvesting directly without requiring additional transformations like in [5]. The application of composite utility was demonstrated by linearizing and iteratively maximizing it using an existing resource allocation that relied on a linear harvesting model, in effect adding the non-linear power harvesting model to the existing algorithm.

REFERENCES

[1] B. Clerckx, R. Zhang, R. Schober, D. W. K. Ng, D. I. Kim, and H. V. Poor, "Fundamentals of Wireless Information and Power Transfer: From RF Energy Harvester Models to Signal and System Designs," *IEEE Journal on Selected Areas in Communications*, vol. 37, no. 1, pp. 4–33, Jan. 2019.

[2] R. P. Ketcham, J. Verdyck, and M. Moonen, "Joint Beamforming and Power Allocation for Multiuser MISO Broadcast Channel SWIPT Employing OFDM," *IEEE Access*, vol. 9, pp. 165 154–165 172, 2021.

[3] S. Wang, L. Ma, and W. Wu, "Joint TS Beamforming and Hybrid TS-PS Receiving Design for SWIPT Systems," *IEEE Access*, vol. 9, pp. 50 686–50 699, 2021.

[4] D. Kumar, O. L. Alcaraz López, S. K. Joshi, and A. Tölli, "Latency-Aware Multi-Antenna SWIPT System With Battery-Constrained Receivers," *IEEE Transactions on Wireless Communications*, vol. 22, no. 5, pp. 3022–3037, May 2023.

[5] E. Boshkovska, D. W. K. Ng, N. Zlatanov, and R. Schober, "Practical Non-Linear Energy Harvesting Model and Resource Allocation for SWIPT Systems," *IEEE Communications Letters*, vol. 19, no. 12, pp. 2082–2085, Dec. 2015.

[6] Jang-Won Lee, R. Mazumdar, and N. Shroff, "Downlink power allocation for multi-class wireless systems," *IEEE/ACM Transactions on Networking*, vol. 13, no. 4, pp. 854–867, Aug. 2005.

[7] E. Boshkovska, D. W. K. Ng, N. Zlatanov, A. Koelpin, and R. Schober, "Robust Resource Allocation for MIMO Wireless Powered Communication Networks Based on a Non-Linear EH Model," *IEEE Transactions on Communications*, vol. 65, no. 5, pp. 1984–1999, May 2017.

[8] E. Boshkovska, N. Zlatanov, L. Dai, D. W. K. Ng, and R. Schober, "Secure SWIPT Networks Based on a Non-Linear Energy Harvesting Model," in *2017 IEEE Wireless Communications and Networking Conference Workshops (WCNCW)*, Mar. 2017, pp. 1–6.

[9] G. Ma, J. Xu, Y. Zeng, and M. R. V. Moghadam, "A Generic Receiver Architecture for MIMO Wireless Power Transfer With Nonlinear Energy Harvesting," *IEEE Signal Processing Letters*, vol. 26, no. 2, pp. 312–316, Feb. 2019.

[10] A. Abdel-Hadi and C. Clancy, "A utility proportional fairness approach for resource allocation in 4G-LTE," in *2014 International Conference on Computing, Networking and Communications (ICNC)*. Honolulu, HI, USA: IEEE, Feb. 2014, pp. 1034–1040.

[11] R. Zhang and C. K. Ho, "MIMO Broadcasting for Simultaneous Wireless Information and Power Transfer," *IEEE Transactions on Wireless Communications*, vol. 12, no. 5, pp. 1989–2001, May 2013.

[12] J. Mo and J. Walrand, "Fair end-to-end window-based congestion control," *IEEE/ACM Transactions on Networking*, vol. 8, no. 5, pp. 556–567, Oct. 2000.

[13] Z. Luo and S. Zhang, "Dynamic Spectrum Management: Complexity and Duality," *IEEE Journal of Selected Topics in Signal Processing*, vol. 2, no. 1, pp. 57–73, Feb. 2008.

[14] J. Brehmer and W. Utschick, "Utility Maximization Strategies in the Multi-User MIMO Downlink," in *2007 International Workshop on Cross Layer Design*. Jinan, China: IEEE, Sep. 2007, pp. 86–90.

[15] J. Brehmer, *Utility Maximization in Nonconvex Wireless Systems*, ser. Foundations in Signal Processing, Communications and Networking. Springer, 2012, vol. 5.

[16] M. Jaggi, "Revisiting Frank-Wolfe: Projection-Free Sparse Convex Optimization," in *Proceedings of the 30th International Conference on International Conference on Machine Learning*, ser. ICML'13, vol. 28. Atlanta, GA, USA: JMLR.org, 2013, pp. 427–435.

[17] R. Jain, D. M. Chiu, and W. R. Hawe, "A Quantitative Measure of Fairness and Discrimination for Resource Allocation in Shared Computer Systems," *ArXiv*, vol. cs.NI/9809099, 1998.